scientific reports

OPEN

Finite element analysis of fixation stability according to reduction position for internal fixation of intertrochanteric fractures

Cheol-Jeong Kim[1], Jung Sub Lee[2], Tae Sik Goh[2], Won Chul Shin[3]✉ & Chiseung Lee[4,5]✉

In recent years, finite element analysis (FEA) has been instrumental in comparing the biomechanical stability of various implants for femur fracture treatment and in studying the advantages and disadvantages of different surgical techniques. This analysis has proven helpful for enhancing clinical treatment outcomes. Therefore, this study aimed to numerically analyze fixed stability according to location using FEA. In this study, a virtual finite element model was created based on a clinically anatomically reduced patient. It incorporated positive and negative support derived from intramedullary and extramedullary reduction from the anteroposterior (AP) view and neutral support from the lateral view. The generated model was analyzed to understand the biomechanical behavior occurring in each region under applied physiological loads. The simulation results of this study showed that the average von Mises stress (AVMS) of the nail when performing intramedullary reduction for femoral fixation was 187% of the anatomical reduction and 171% of the extramedullary reduction, and individually up to 2.5 times higher. In other words, intramedullary reduction had a very high possibility of fixation failure compared to other reduction methods. This risk is amplified significantly, especially in situations where bone strength is compromised due to factors such as old age or osteoporosis, which substantially affects the stability of fixation. Extramedullary reduction, when appropriately positioned, demonstrates greater stability than anatomical reduction. It exhibits stable fixation even in scenarios with diminished bone strength. In instances in which the bone density was low in the support position, as observed in the lateral view, the AVMS on the nail appeared to be relatively low, particularly in cases of positive support. Additionally, the femur experienced lower equivalent stress only in the extramedullary reduction-negative position. Moreover, by comparing different reduction methods and bone stiffness values using the same femoral shape, this study offers insights into the selection of appropriate reduction methods. These insights could significantly inform decision making regarding surgical strategies for intertrochanteric fractures.

Intertrochanteric fractures represent approximately 50% of hip fractures. These fractures primarily affect older patients with osteoporosis and reduced bone density. Even after internal fixation for fracture treatment, the occurrence of complications remains high, contributing to a significant 1-year post-surgery mortality rate ranging between 14 and 36%[1]. Given the multifaceted medical conditions common among older patients, minimizing the need for repeated reductions during surgery is imperative to reduce the surgical duration and occurrence of surgical mishaps[2].

[1]Department of Biomedical Engineering, Graduate School, and University Research Park, Pusan National University, Busan 46241, Republic of Korea. [2]Department of Orthopaedic Surgery, School of Medicine, Biomedical Research Institute, Pusan National University, Pusan National University Hospital, Busan 49241, Republic of Korea. [3]Department of Orthopaedic Surgery, Pusan National University School of Medicine, Pusan National University Yangsan Hospital, Yangsan 50612, Republic of Korea. [4]Department of Biomedical Engineering, School of Medicine, Pusan National University, Busan 49241, Republic of Korea. [5]Biomedical Research Institute, Pusan National University Hospital, Busan 49241, Republic of Korea. ✉email: dreami3e5t@pusan.ac.kr; victorich@pusan.ac.kr

Two types of implants are commonly used for internal fixation of intertrochanteric fractures: proximal femoral nails and sliding hip screws. Proximal femoral nails offer several advantages, including a telescopic effect at the fracture site, preservation of the lever arm, minimal invasiveness, and a straightforward surgical technique. Due to the abovementioned benefits, they are preferred for treating femoral intertrochanteric fractures in older patients, thereby reducing postoperative complications and enabling quicker mobility[3].

Nevertheless, despite the use of proximal femoral nails, issues such as nonunion, internal fixation fractures, and blade/screw cut-outs persist[4,5]. Intertrochanteric fractures are categorized into stable and unstable based on the fracture fragment and fracture line direction. The overall failure rate for unstable fractures reportedly ranges between 3 and 12%, which is higher than that for stable fractures[6,7].

Evaluation results at times may exhibit inconsistency between the anteroposterior (AP) and lateral views of intraoperative fluoroscopy, which increases the difficulty for surgeons in making accurate judgments[8,9]. Among these critical factors, only reduction and blade/screw positions can be controlled. Therefore, fracture reduction and implant placement play a crucial role in surgical success. Anatomical reduction, in which both AP and side views achieve neural support, is generally considered the primary goal of fracture reduction. The actual quality of fracture reduction can be categorized into three types: neutral, positive, and negative. This categorization arises due to the rarity of achieving precise anatomical reduction according to the anatomical codex. The entity termed "anatomic reduction" encompasses three different conditions: the exact anatomic cortex-to-cortex position, a slightly positive position, and a slightly negative position[10].

Kawamura reported that among extramedullary and intramedullary reductions classified based on the fixation location of the head-neck and medial cortex of the femur in AP view, extramedullary reduction exhibited better outcomes[3]. However, this result stemmed from evaluation of two-dimensional displacement alone under uniaxial loading conditions using 'imitation osteoporotic bone material', necessitating additional biomechanical analysis. Additionally, other reports indicate that the anterior femoral neck cortex, located posteriorly in the lateral view, poses a higher risk of excessive lag screw slippage than the distal anterior position. However, biomechanical evidence supporting this clinical advantage is lacking[11].

In recent years, finite element analysis (FEA) has been instrumental in comparing the biomechanical stability of various implants for femur fracture treatment and in studying the advantages and disadvantages of different surgical techniques[12]. This analysis has proven helpful for enhancing clinical treatment outcomes. Therefore, this study aimed to numerically analyze fixed stability according to location using FEA. In this study, a virtual finite element model was created based on a clinically anatomically reduced patient according to the flowchart in Fig. 1. It incorporated positive and negative support derived from intramedullary and extramedullary reduction from the AP view and neutral support from the lateral view. The generated model was analyzed to understand the biomechanical behavior occurring in each region under applied physiological loads.

Materials and methods

This study implemented finite element models for intertrochanteric fractures, encompassing anatomical, intramedullary, and extramedullary reductions based on the fracture reduction positions. Their mechanical stability under physiological loads was evaluated using the Finite Element Method (FEM). Medical imaging included in this study was approved with patient consent and by the Institutional Review Board of Pusan National University Yangsan Hospital.
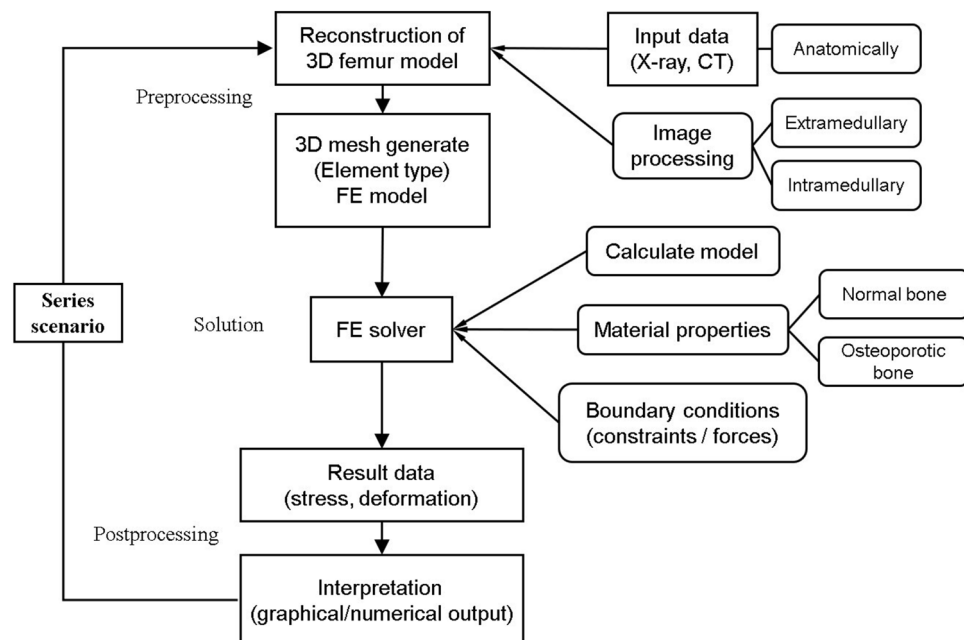

Figure 1. Flowchart of series FEA for analysis of biomechanical behavior of the femur.

Medical image conversion

CT images selected for the construction of finite element model adhered to specific criteria. First, the patient underwent internal fixation surgery using a proximal femoral nail to treat an intertrochanteric fracture at the author's affiliated hospital. Second, the fracture pattern was categorized as corresponding to A.1 according to the AO Foundation/Orthopedic Trauma Association (AO/OTA) classification criteria[13]. Finally, the fracture reduction mode constituted anatomical reduction. A finite element model was generated based on post-surgery images of the selected patient (86 years old, female, 165 cm, and 66 kg), excluding fragments not involved in load support resulting from the fracture.

CT data scans were conducted using Revolution (GE Healthcare, Wisconsin, USA) to construct a three-dimensional model by extracting the regions of interest (ROI) containing the fracture site and implants from CT scan images of 512 × 512 resolution with 0.625 mm spacing. CT images were produced in the Digital Imaging and Communications in Medicine (DICOM) format, and the femoral and femoral head surfaces were reconstructed using CT slice images generated through the Mimics program (Version 23.0, Materialise NV, Leuven, Belgium). The SpaceClaim software integrated into ANSYS was used to create and modify the solid body of the femoral condyle implant. The finite element model analysis was performed using the ANSYS Workbench.

Fracture reduction classification

Figure 2 is a 3D modeling of the shape according to the location of femur fracture reduction for each case. The location of the geometric reduction of the intertrochanteric fracture in AP and lateral views is explained as follows: Positive support: This stable fracture reduction facilitated early patient mobilization. Neutral support can transition to positive or negative support after early weight-bearing exercises. In the AP view, if the medial cortex of the head-neck fragment is slightly superomedial to the upper medial edge of the femoral shaft, it corresponds to extramedullary reduction, representing positive support. Conversely, if the medial cortex of the head-neck fragment is positioned lateral to the upper medial edge of the shaft fragment, it signifies intramedullary reduction
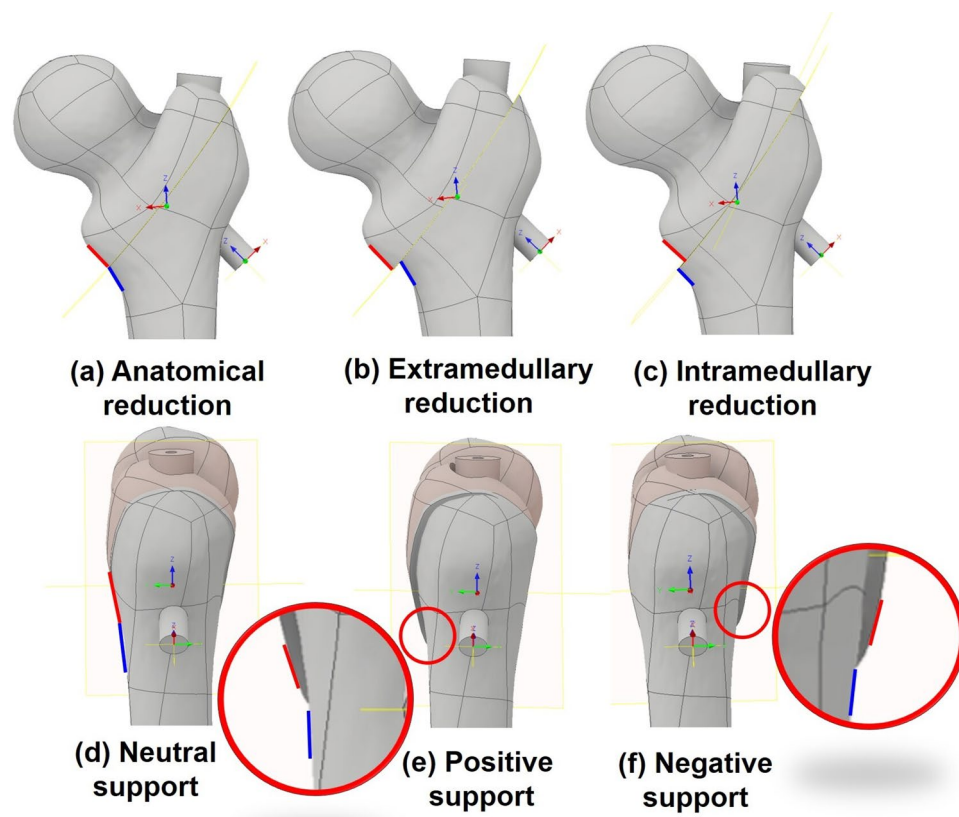

Figure 2. Different types of AP and lateral views for fracture reduction of intertrochanteric hip fractures. (**a**) The medial cortex of the head and neck fragment (red) is in smooth contact with the medial cortex of the femur (blue), anatomical reduction. (**b**) In the AP view, the medial cortex of the head and neck fragment (red) is located slightly medial to the upper medial edge of the femoral shaft (blue), extramedullary reduction, (**c**) the medial cortex of the head-neck fragment (red) is laterally displaced relative to the upper medial edge of the axial fragment (blue), intramedullary reduction. (**d**) In lateral view, the entire cortex is in smooth contact, neutral support, (**e**) the head and neck cortex (red) is classified as benign if it is displaced anteriorly by more than half the cortical thickness, positive support, (**f**) displaced posteriorly by more than half of the cortical thickness, negative support.

associated with negative–positive support. Anatomical reduction is achieved when the medial cortex of the head-neck fragment makes smooth contact with the medial cortex of the femoral shaft[8].

Boundary condition

To simulate the load effects of the patient's body weight and abductor muscle, the femur FEA study referenced multiple sources[14,15]. Wang observed an imitation biomaterial model fracturing at 2378.5 N, primarily at an angle of approximately 20° to the vertical axis. The study verified that the stress concentration points in the finite element model aligned with similar biological experimental results under uniaxial loading[16].

To simulate normal walking, the load direction and magnitude received by a single leg were set at 20° relative to the vertical axis, as illustrated in Fig. 3. According to Kwak's report, the hip joint reaction force applied a load equivalent to 300% of the body weight to the femoral head, whereas the abductor muscle exerted a load equivalent to 100% of the body weight. Consequently, 1942.2 N, three times the 647.4 N corresponding to the patient's weight of 66 kg in this study, was applied to the femoral head, and 647.4 N, representing the abductor muscle load, was applied in the opposite direction.

The frictional coefficient was set to 0.42 for the nail and proximal bone interface and to 0.46 for interactions between the proximal and distal bone fragments. Contact conditions were implemented using a frictionless of between the lag screw and proximal bone, between nail and lag screw to facilitate optimal movement. Bonded contact condition was applied in this study, assuming full constraints between distal bone fragments and the lag screw[18].

Material properties

Ethical constraints prevent the direct study of living bone through experiments, and cadaveric bone cannot entirely replicate real osteocytes lesions[16]. To facilitate the analysis, a titanium alloy (TI6Al4V) with Young's modulus of 113.8 GPa and Poisson ratio of 0.34 was used for the nail[18].

The elastic modulus (E) of the cancellous bones of the femur were referenced from data from a study that performed similar simulations, where the elastic modulus of normal and osteoporotic bones were applied to the series analysis[15,19,20]. The Poisson's ratio for both types of bone was set to 0.2[18]. Previous studies on human femur properties confirmed the yield stress of cancellous bone as 133.6 MPa and cortical bone as 153 MPa, which were applied in this analysis[21,22].

The yield stress of the titanium alloy was computed using the titanium alloy data incorporated into ANSYS Workbench. The program provided a yield stress value of 930 MPa, which was validated and found to be in concordance with a study on the material properties of TI6Al4V[23], and these material properties are summarized in Table 1.

Finite element analysis

In this study, finite element models were generated based on a patient who underwent anatomical reduction for an intertrochanteric fracture. Series analyses were conducted for intramedullary and extramedullary reductions in the AP view and positive, negative, and neutral supports in the lateral view. As illustrated in Fig. 4, the fracture reduction simulations were performed by adjusting the position of the femoral head at regular intervals.

In the AP view, movements up to 3 mm were performed in increments of 1 mm for both intramedullary and extramedullary reductions. Similarly, in the lateral view, movements were made in the positive and negative support directions at 1 mm intervals, also reaching a maximum of 3 mm. This resulted in a total of 49 series simulations. The fracture shape replicated the actual fracture site in the patient. To fix intertrochanteric femoral fractures, an intramedullary implant with a single lag screw was used. The total nail length was 200 mm, with an outer thread diameter of 8.8 mm and a top diameter of 15.8 mm. The lag screw, which penetrated the fracture site and secured the femoral head, formed a 125° angle with the nail and measured 100 mm in length and 9.5 mm in diameter.

Physiological loads were applied to the 49scenario analysis model, assuming normal bone density, to calculate the maximum von Mises stress (MVMS) at the implant, femur, and fracture surfaces. Nine additional simulations were conducted considering the osteoporotic properties, specifically selecting the maximum displacement case of anatomical reduction and other reduction methods. This analysis aimed to assess the fixation stability and risk of fixation failure by comparing the MVMS at the implant and femur with the yield strength of the fixation device.

To ensure the reliability of the finite element analysis results in this study, a mesh convergence test was performed. Using the automatic mesh generation function of the ANSYS program used for the analysis, finite element models with global mesh sizes of 1 mm, 2 mm, 3 mm, 4 mm, and 5 mm were created, following the same method as previously employed[24]. The analysis case is anatomical reduction-neutral support, and other cases such as extramedullary reduction and intramedullary reduction are derived from the geometry of anatomical reduction-neutral support, so mesh convergence was tested for one case. Equivalent stress on the entire model was measured under the same loading conditions as in the series analysis, and the mesh size that increased by within 5% based on the value calculated with the fine mesh size was selected as the optimal element size in line with earlier studies[15,25]. To confirm the closest result within 5% of the fine mesh results, an element size of 2.2 mm was added. Figure 5 summarizes the equivalent stress, deformation, number of elements, and element quality for each mesh size. Considering the difference in equivalent stress, number of elements, and element quality comprehensively, it was determined that an element size of 2 mm is optimized size, and this was applied to all cases for the analysis, consistent with previous findings[13,20].
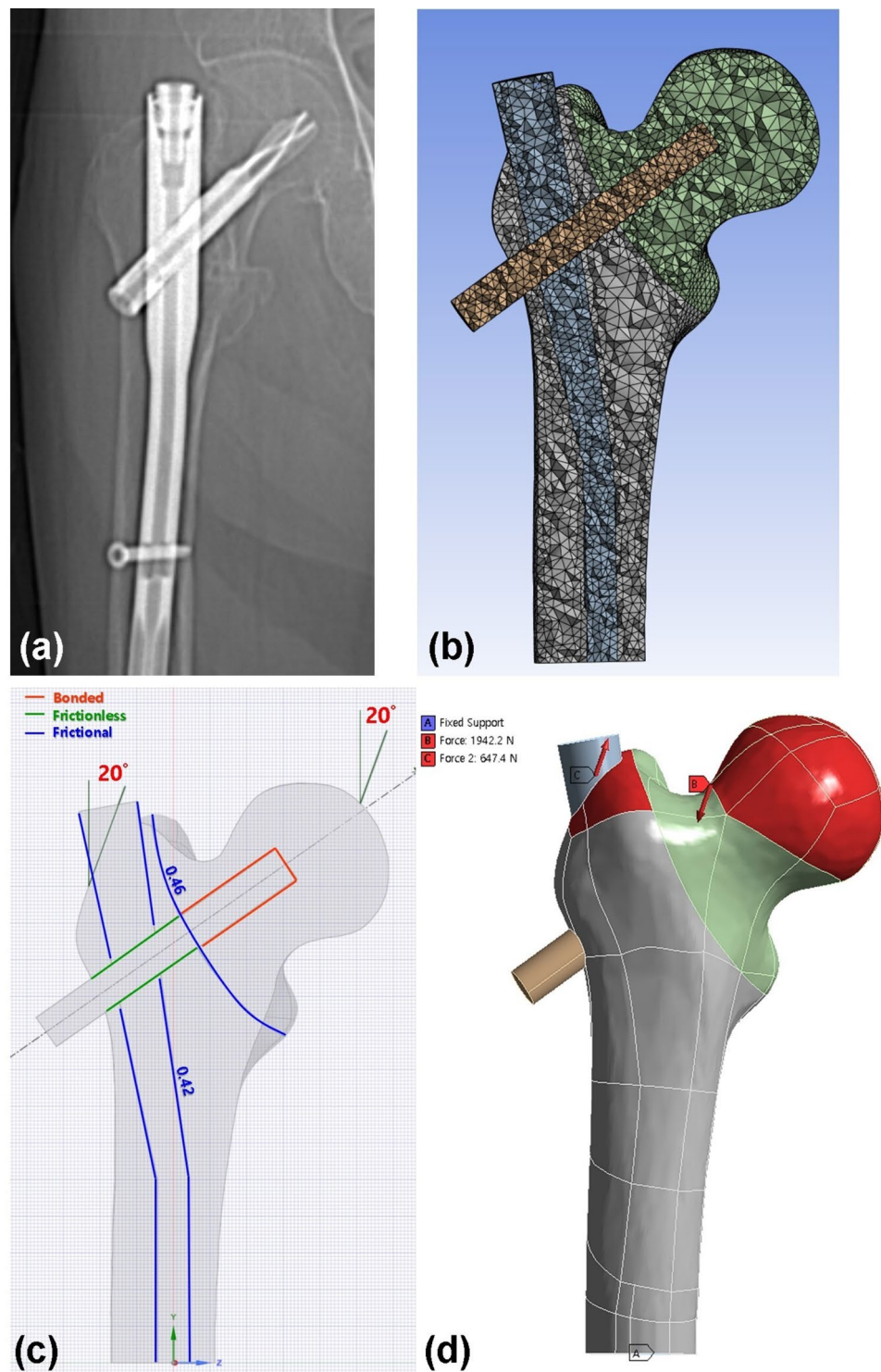
Figure 3. Internal fixation with implants was performed on a fractured femur, (**a**) X-ray AP view. (**b**) Mesh image of the cross-section of the finite element model (consisting of tetrahedral elements[17]). (**c**) Contact conditions between the femur and the internally fixed nail and lag screw. (**d**) Loading condition of the analysis model. Hip joint force, 1942.2 N (body weight × 300%); abductor muscle force, 647.4 N (body weight × 100%).

Consent statement

The study was conducted according to the guidelines of the Declaration of Helsinki and Informed consent was waived by the Institutional Review Board of Pusan National University Yangsan Hospital (IRB No. 05-2023-022).

Material		Element type (ANSYS)	Young's modulus (MPa)	Yield stress (MPa)	Poisson's ratio
Femur	Cortical bone	8-node structural shell (SHELL281)	17,000[18]	153[22]	0.3[18]
	Cancellous bone—normal	10-node solid element (SOLID187)	966.8[15,19]	133.6[21]	0.2[18]
	Osteoporotic		674.4	93.2	
Nail	Ti6Al4V	10-node solid element (SOLID187)	113,800[18]	930[23]	0.34[18]
Lag screw		10-node solid element (SOLID187)			

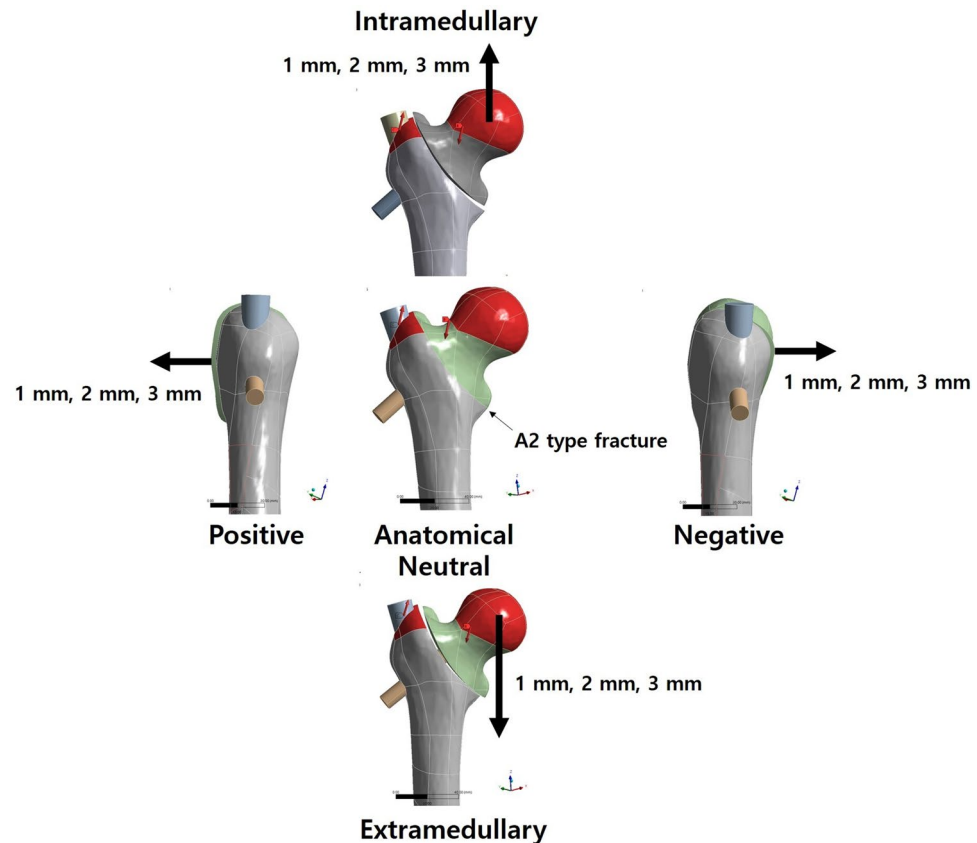**Table 1.** Material properties of human femur.

Figure 4. Simulation scenario for each case of femur fracture reduction.

Results

Implant stress and femur stress

Figure 6 shows the MVMS of the nail with respect to the reduction method for intertrochanteric fractures under normal bone. Metallic implants possess significantly higher moduli and consequently bear a substantial portion of the physiological load. This discrepancy in load sharing between the implant and bone leads to stress shielding, which deprives the bone of essential mechanical stimulus required for its maintenance. Thus, it was anticipated that lower stress at the interface between the nail and bone would indicate a more appropriate fracture reduction method. These expectations were based on calculating the MVMS of the implant corresponding to the reduction position, assuming that the reduction method yielding the lowest amount of stress would be the most stable. Conversely, higher MVMS signifies a fracture reduction method, increasing the risk of fixation failure due to nail deformation and breakage, and the possibility of femoral fracture due to stress shielding.

The highest equivalent stress on the nail was observed in intramedullary reduction (3 mm) in the AP view and positive support (3 mm) in the lateral view. A slight difference of approximately 18 MPa was noted, even with a negative support (3 mm). Regardless of the change in the material view position, the overall AVMS for intramedullary reduction (3 mm) was 856.3 MPa, which was significantly higher than that in other cases. 1 mm change in the intramedullary reduction direction led to 26.4%, 93%, and 163.2% increase in equivalent stress, respectively, in comparison to anatomical reduction. Conversely, the equivalent stress change rates for extramedullary reduction in the opposite direction were 5.5%, 18.5%, and 27.2%, respectively. This implies that the equivalent stress was higher with a 3 mm extramedullary reduction than with a 1 mm intramedullary reduction. In the lateral view, the equivalent stress decreased by 0.2% for anatomical reduction in the 1 mm positive support direction,
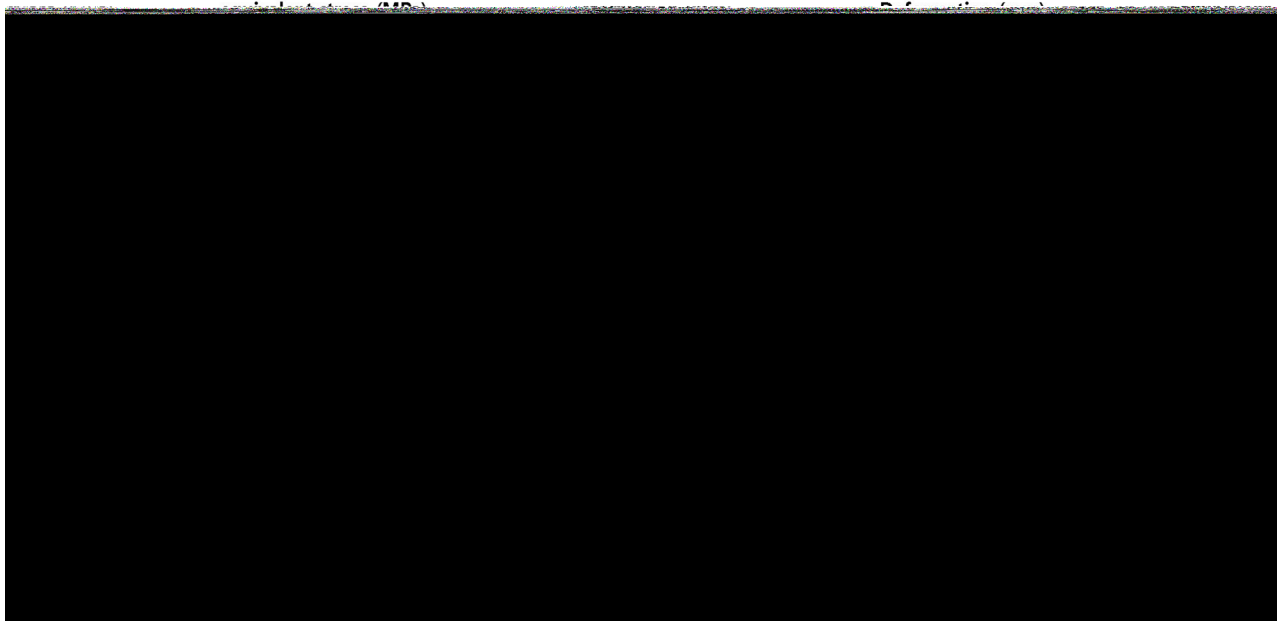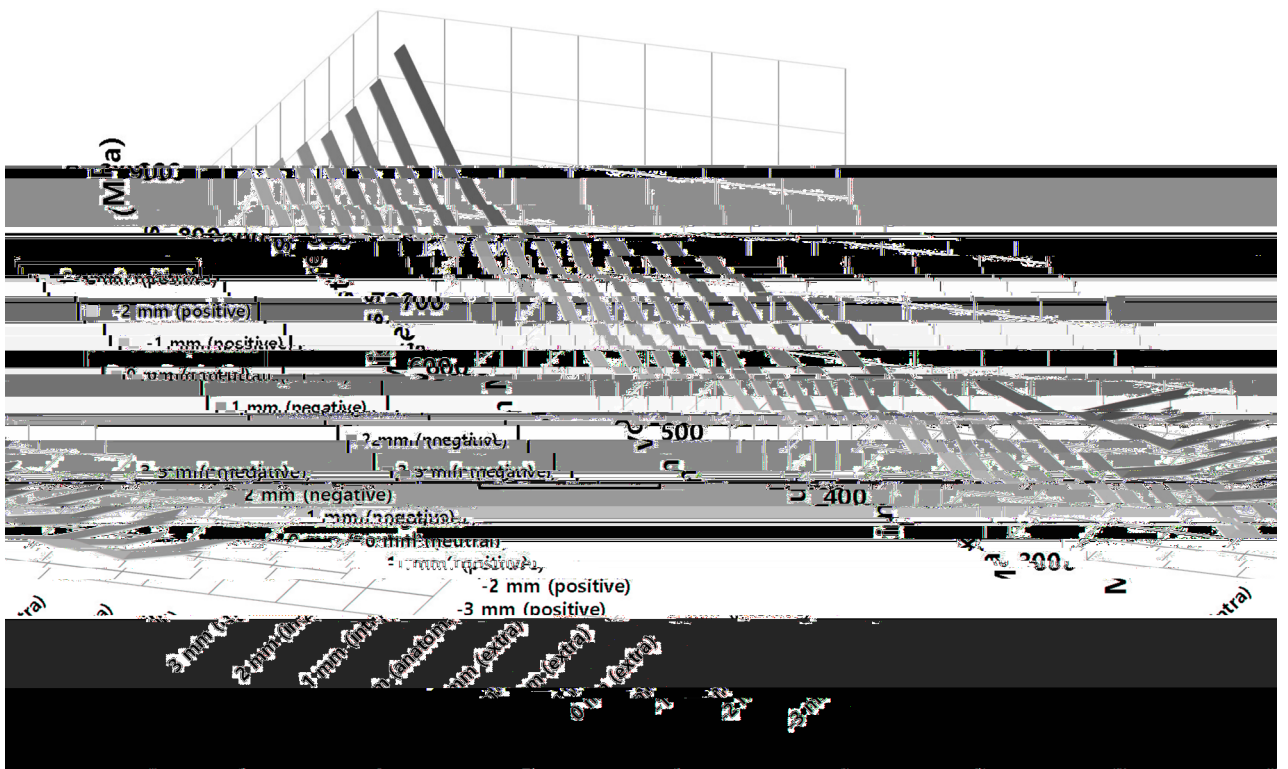
Figure 5. Mesh convergence with equivalent stress and total deformation analysis at anatomical reduction and neutral support position.

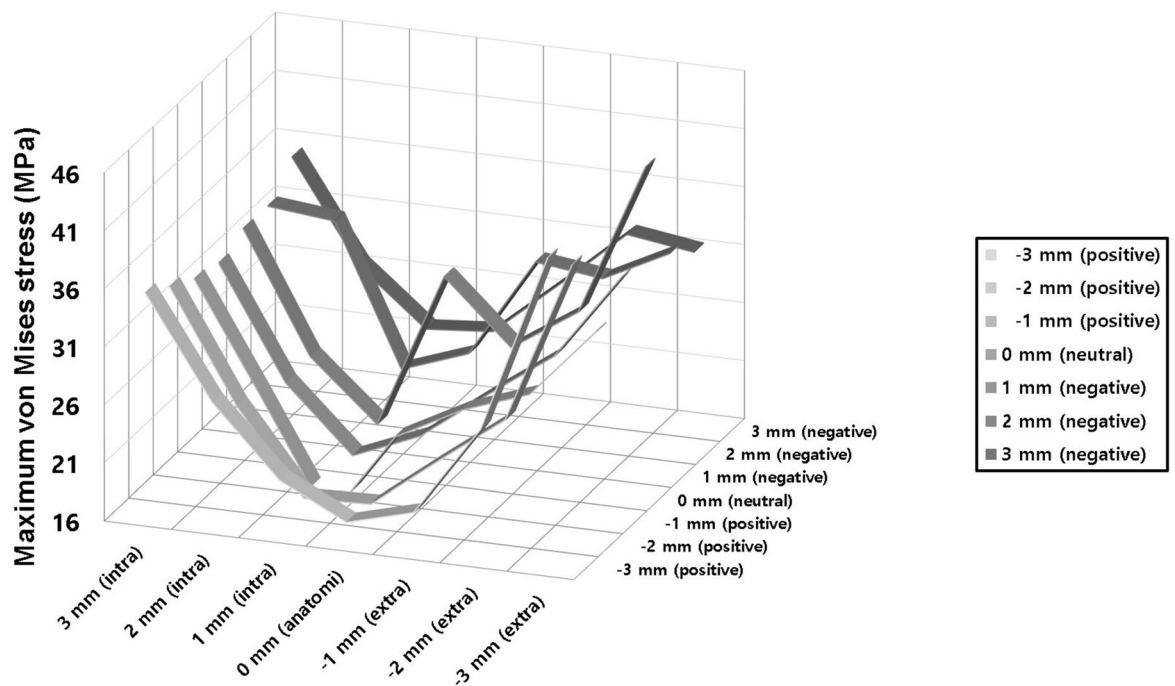| 3 mm (negative)	average		-3 mm (positive)	-2 mm (positive)	-1 mm (positive)	0 mm (neutral)	1 mm (negative)	2 mm (negative)
865.14	856.3	3 mm (intra)	**883.11**	865.83	855.35	838.02	839.69	847.24
660.8	626.6	2 mm (intra)	627.97	626.51	620.65	614.71	608.87	626.94
590.57	445.6	1 mm (intra)	479.75	457.3	445.05	402.59	406.03	455.66
388.5	343.2	0 mm (anatomi)	366.93	322.64	**317.7**	318.44	319.05	369.07
344.98	339.6	-1 mm (extra)	348.1	335.75	334.25	336.11	337.71	340
380.84	374.6	-2 mm (extra)	369.74	368.99	372.24	377.22	375.93	377.51
412.45	407.8	-3 mm (extra)	402.93	403.51	404.76	405.19	407.41	418.06

Figure 6. Maximum von Mises stress of nail at normal bone.

whereas the most substantial increase was observed in the 3 mm negative support direction, which increased by 22%. In the case of 2 mm extramedullary reduction, 2 mm positive support exhibited the most considerable reduction rate among all cases, which decreased by 2.2%. In contrast, for intramedullary reduction (1 mm) and 3 mm negative support, the equivalent stress increase rate was 26.2%, demonstrating the highest increase due to lateral movement. The extramedullary reduction (1 mm), which exhibited the lowest AVMS with lateral direction changes, was 339.6 MPa. Comparatively, anatomical reduction averaged 343.2 MPa, showing a slight difference. However, ultimately, extramedullary reduction depicted the lowest AVMS.

Figure 7 shows the MVMS within the fracture surface based on fracture reduction method for intertrochanteric fractures under normal bone. Notably, the equivalent stress observed on the femur exhibited a slightly different trend than that on the nail. While the highest equivalent stress occurred in the nail due to intramedullary reduction (3 mm), in the femur, it was observed with extramedullary reduction (3 mm). Furthermore, while the nail exhibited a somewhat higher deviation in equivalent stress generation, the femur displayed a low maximum–minimum stress difference of about 23 MPa. Even when considering the variances in physical properties between titanium alloy and human bone, stress variation on femur remained relatively consistent across each case. The AVMS across all cases in the lateral view was 20.2 MPa, with the lowest stress observed during intramedullary reduction (1 mm). This outcome contrasts with the fact that the nail experienced the lowest AVMS during extramedullary reduction (1 mm). To further analyze the results, the ratio of equivalent stress from the FEA in this study was calculated in comparison with the compressive ultimate stress of the femoral cortical bone[26]. This analysis revealed that 13.2% of the ultimate compressive stress on the cortical bone was observed during intramedullary reduction (1 mm), whereas 17% occurred during extramedullary reduction (1 mm). Lower stress levels were observed in intramedullary reduction than in extramedullary reduction (1 mm). Additionally, from the lateral view, it was confirmed that reduced amount of stress occurred when supported in the positive direction than when supported in the negative direction, aligning with the equivalent stress trend observed in the nail.

Fracture region stress

Figure 8 shows the stress contour occurring on the fracture surface with respect to the fracture reduction method for intertrochanteric fractures with normal bone. The stress values at the fracture surface, as shown in Fig. 7, closely resembled the MVMS experienced by the femur in each case. These results suggested that a significant portion of the maximum stress generated by load-bearing post-fracture surgery was concentrated at the fracture

	-3 mm (positive)	-2 mm (positive)	-1 mm (positive)	0 mm (neutral)	1 mm (negative)	2 mm (negative)	3 mm (negative)	average
3 mm (intra)	35.411	33.964	32.676	32.072	33.071	32.999	35.285	33.6
2 mm (intra)	26.685	24.388	23.184	22.423	22.722	32.427	26.595	25.5
1 mm (intra)	20.717	17.182	13.397	16.872	17.595	20.362	21.853	18.3
0 mm (anatomi)	17.821	17.388	21.195	19.254	31.038	22.427	22.357	21.6
-1 mm (extra)	19.377	21.803	24.224	23.515	25.64	31.05	27.172	24.7
-2 mm (extra)	27.248	26.059	26.284	27.583	29.421	30.329	32.173	28.4
-3 mm (extra)	42.766	40.177	32.45	35.06	42.636	33.22	31.357	36.8

Figure 7. Maximum von Mises stress of fracture surface at normal bone.

surface. In addition, the stress distribution direction was confirmed by examining the stress contour at the fracture surface.

Given the challenge of determining whether aligning the physiological load and load transfer directions of the fracture surface benefits fixation stability, the primary focus was to analyze the directionality of the load distribution. During anatomical reduction, the neutral support was slightly directed towards the rear of the body, positive support was approximately 45° towards the rear, and negative support was nearly towards the center of the nail. Notably, in anatomical reduction, the physiological load direction closely mirrored the direction of stress distribution.

Intramedullary reduction showed stress distribution tendency similar to that of anatomical reduction. However, in extramedullary reduction, irrespective of whether the lateral view was neutral, positive, or negative, stress distribution was consistently directed towards the rear of the body.
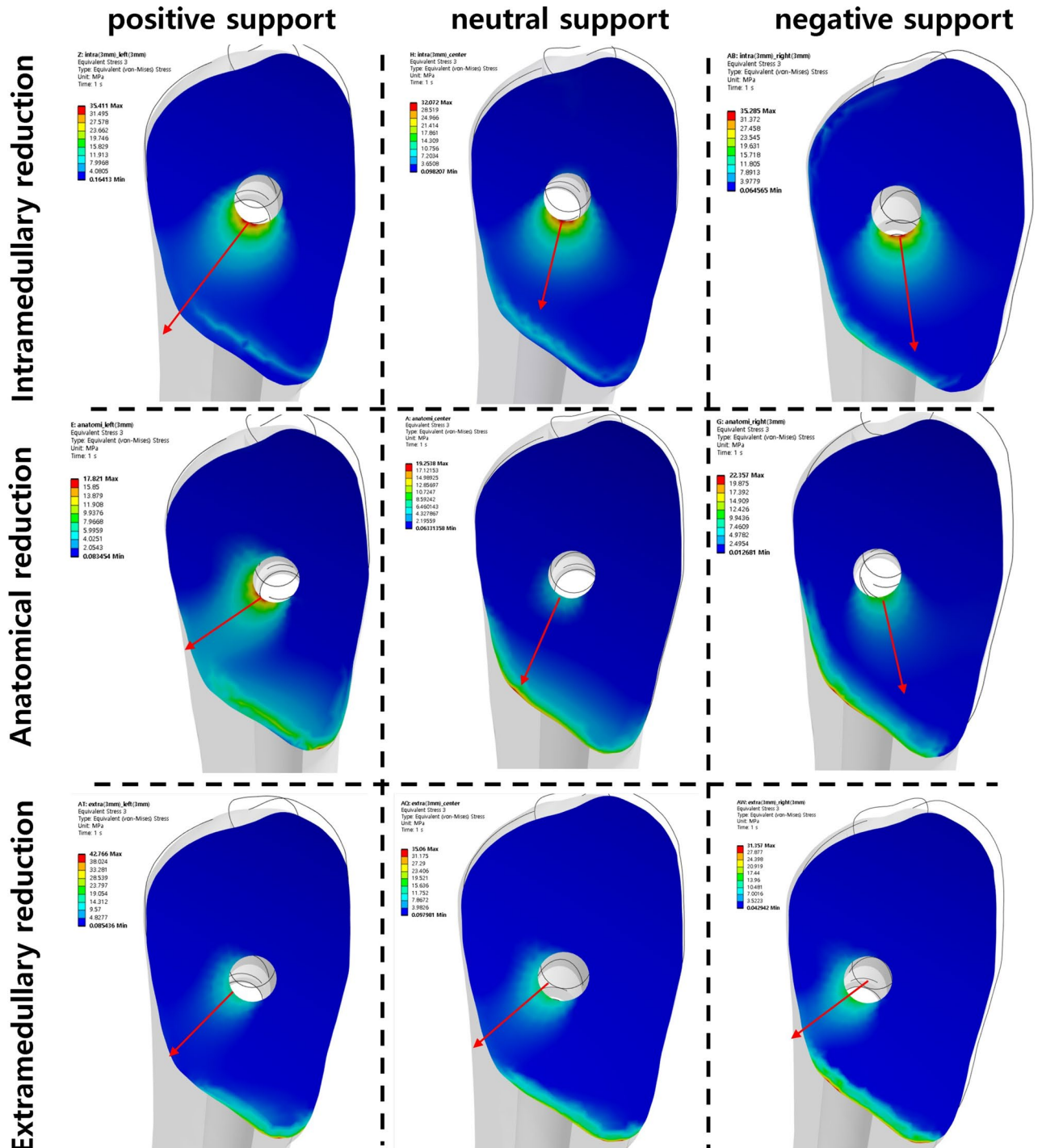

Figure 8. Fracture surface equivalent stress contour for each reduction and support position.

In case of osteoporotic bones

Figure 9a shows the MVMS of the nail in a scenario in which the reduction position represents maximum displacement when fixing an intertrochanteric fracture in an osteoporotic bone. The AVMS for anatomical reduction was 406.7 MPa, whereas that for extramedullary reduction was 455.2 MPa. Intramedullary reduction recorded the highest AVMS at 923.8 MPa, marking 7.9% increase compared with normal bone density scenarios. The lowest AVMS was 339.6 MPa under normal bone density conditions, whereas in the osteoporotic state, it measured 406.7 MPa, signifying an increase of 34%. Interestingly, regardless of the bone density, intramedullary reduction exhibited the highest AVMS, whereas anatomical reduction showed the lowest amount of stress.

Figure 9b illustrates the equivalent stress experienced by the fracture surface in a scenario in which the reduction position represents maximum displacement when fixing an intertrochanteric fracture in an osteoporotic bone. The AVMS observed for anatomical reduction was 20.6 MPa, whereas that for intramedullary reduction was 27.1 MPa. Extramedullary reduction registered the highest AVMS at 33.7 MPa, marking 8.3% decrease compared with that observed in scenarios with normal bone density. In the case of normal bone density, the lowest AVMS encountered by the femur was 18.3 MPa at anatomical reduction. Conversely, under osteoporotic conditions, there was a slight decrease 11.2%. Interestingly, unlike in the nail scenario, regardless of the bone density, extramedullary reduction displayed the highest AVMS, and in the osteoporotic state, the stress experienced was lower than that in the normal bone density state. In most instances, stress observed on the fracture surface exhibited an inverse trend to that of the nail, with the equivalent stress in osteoporotic bone demonstrating an average decrease of 12.7% compared to the normal state. The most reduction occurred in positive support of intramedullary reduction, which demonstrated a decrease by 24.1% from 33.6 to 27.1 MPa. Conversely, in cases of increased stress, there was a 5% decrease from 20.6 to 21.6 MPa due to the neutral support of anatomical reduction; however, this difference was not significant.

Discussion

This study conducted a FEA to assess fixation stability based on reduction location following surgical intervention for femoral intertrochanteric fractures. In clinical practice, anatomical reduction and neutral supports is generally regarded as yielding optimal outcomes in both AP and lateral views. However, controversies persist regarding the most stable reduction method, even in empirical clinical studies. Decision analysis models, such as those used by Lee[27], indicate that intramedullary nailing may offer an enhanced quality of life for patients with intertrochanteric fractures. However, reliance on such decision analyses lacks objectivity as the final outcomes rely heavily on the chosen literature and validity of utilities used to construct the model. Biomechanical research by Schipper suggested the feasibility of immediate[28], unrestricted mobility post-surgery under full weight-bearing conditions, while cautioning against the use of intramedullary reduction for trochanteric fractures. Additionally, Jia's findings indicated that accurate prediction of cortex support situations becomes possible when the images of AP and lateral views coincide[8]. Their study emphasized the importance of verifying cortical support for both views, striving for positive support, and ensuring that the lateral location can facilitate positive support. In alignment with these considerations, our study segmented the reduction location variables according to the AP and lateral views. Reduction positions were categorized into three methods, anatomical, intramedullary, and
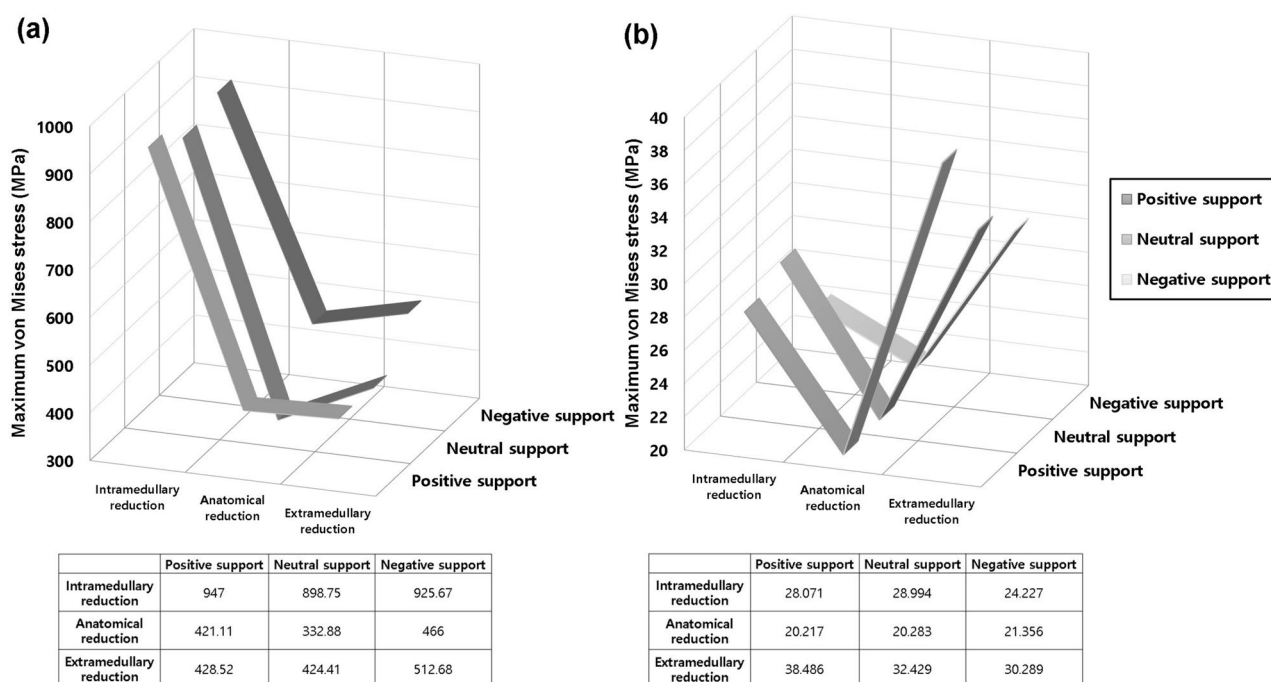

	Positive support	Neutral support	Negative support
Intramedullary reduction	947	898.75	925.67
Anatomical reduction	421.11	332.88	466
Extramedullary reduction	428.52	424.41	512.68

	Positive support	Neutral support	Negative support
Intramedullary reduction	28.071	28.994	24.227
Anatomical reduction	20.217	20.283	21.356
Extramedullary reduction	38.486	32.429	30.289

Figure 9. Maximum von Mises stress of (**a**) nail, (**b**) fracture surface at osteoporotic bone.

extramedullary in the AP view, whereas the support positions were neutral, positive, and negative in the lateral view. Thus, this study compared the stability of different types of reduction in patients who underwent anatomical reduction after fixation surgery for intertrochanteric femoral fracture.

Kawamura's study highlighted significant differences between the "intramedullary" and "extramedullary" reduction patterns[3]. Specifically, it reported that "intramedullary" reduction exhibited larger blade telescoping and distal screw hole diameters compared to "extramedullary" reduction. Biomechanical testing revealed that the "extramedullary" reduction pattern improved stability and reduced slipping, confirming the instability associated with "intramedullary" reduction pattern. These findings are consistent with our study, where the highest MVMS in the nail was observed in "intramedullary" reduction by 3 mm in the average AP view and "positive support" by 3 mm in the lateral view. Notably, MVMS increased significantly by more than 200 MPa for every 1 mm change in reduction location in the "intramedullary" reduction method. Therefore, based on the results obtained through FEA, it is imperative to avoid "intramedullary" reduction or choose a location with minimal displacement to mitigate the risk of fixation failure attributed to nail deformation or breakage. Of note, particularly concerning is the rapid stress escalation at displacements of ≥ 2 mm in "intramedullary" reduction, warranting the selection of reduction location of ≤ 1 mm to minimize the likelihood of nail breakage.

Surprisingly, the lowest amount of AVMS observed on the nail was not in the case of "anatomical" reduction but rather in "extramedullary" reduction by 1 mm. In some instances of "extramedullary" reduction, the equivalent stress was even lower than that observed in "anatomical" reduction. However, when the reduction position exceeded 2 mm, "anatomical" reduction showed slightly higher AVMS compared to "extramedullary" reduction. Nonetheless, "extramedullary" reduction demonstrated less pronounced stress changes than the stress variations observed in "intramedullary" reduction. Therefore, when opting for "extramedullary" reduction, significant restrictions based on location are not expected. However, it is important to note that despite the lower AVMS on the nail, "extramedullary" reduction resulted in higher AVMS on femur compared to "intramedullary" reduction. Thus, to avoid the risk of nail breakage, it is advisable to limit the reduction position to ≤ 2 mm, even in the case of "extramedullary" reduction. A notable about 1.8 times increase was observed when comparing the AVMS of "extramedullary" reduction by 2 mm to "anatomical" reduction. A little differently from that "intramedullary" reduction by 2 mm demonstrated 9.2% increase in AVMS compared to "anatomical" reduction. To balance the risks associated with both nail breakage and potential femur damage, it is imperative to consider selecting displacement within 1 mm for "intramedullary" reduction and within 2 mm for "extramedullary" reduction.

In the lateral view, no significant changes were observed in equivalent stress concerning neutral, positive, and negative supports. However, in cases of negative support in both anatomical and extramedullary reductions, slightly higher average stress levels were observed than in other scenarios. Particularly, in instances involving osteoporotic bone conditions, the load exerted on the nail increases, which can potentially lead to higher fixation failure rates attributed to nail deformation or breakage. Based on the findings of FEA, it is advisable to limit the reduction position to less than 1 mm for "intramedullary" reduction and less than 2 mm for negative support to mitigate the fixation failure risk. Similar findings were observed in a study by Liang et al., who reported that positive support and anatomical reduction exhibited superior biomechanical stability compared to negative support in AO31A1 intertrochanteric fractures. Despite the relatively low difference in stress levels (18.5 MPa) at the fracture surface, considering the ultimate stress of human femur properties in a 60-year-old individual, which stands at 195 MPa[26], with longitudinal compressive stress at 193 MPa and transverse compressive stress at 133 MPa[29], even minimal stress levels warrant attention. Anatomical reduction exhibited an AVMS of 11.1% of the ultimate stress, which corresponded to 12.8% of the longitudinal compressive strength and 21.4% of the horizontal compressive strength. In contrast, extramedullary reduction, where the highest stress was observed (AVMS of 3 mm), demonstrated a stress ratio of 18.9% of the ultimate stress, reflecting higher stress levels equivalent to 19.1% of the longitudinal compressive strength and 27.7% of the horizontal compressive strength. Using FEA, we conducted a scenario analysis focusing on osteoporotic bone conditions using the same femur geometry. Given that most femoral intertrochanteric fractures occur in older patients, it is noteworthy that bone stiffness in patients with osteoporosis and in older patients tends to be lower than that in normal bone conditions. Initially, all analyses were conducted by applying bone strength parameters in a normal state. Representative cases of low bone density, akin to osteoporosis, were specifically examined. However, representing the bone condition of patients with osteoporosis and older adults based solely on elasticity coefficients poses challenges due to inadequate data on bone density changes related to age and disease.

Figure 10 presents a comparative graph derived from the FEA of normal bone density and osteoporotic bone, emphasizing the impact of bone stiffness on fixation stability by evaluating the equivalent stress on nail and femur according to the reduction type. Overall, the equivalent stress experienced by the nail exhibited an average increase of 10.7% when fixing osteoporotic bone compared to a normal femur. The most significant increase was observed in the extramedullary reduction-negative support, which escalated by 24.3% to 412.6 MPa in normal conditions and by 512.7 MPa in osteoporotic bone. Conversely, the reduction method with the least influence on changes in bone strength was anatomical reduction-neutral support, showcasing an increase of 4.5% to 318.4 MPa in normal conditions and 332.9 MPa in osteoporotic bones. Notably, similar reduction methods demonstrated markedly distinct stress trends contingent on the lateral view. Average of the stress levels on the nail revealed that anatomical intra-, extra- reductions increased the equivalent stress by an average of 13.1%, 11.8%, and 7.2%, respectively. Among these scenarios, the extramedullary reduction-negative support exhibited the highest increase in stress. Conversely, the extramedullary reduction-positive support demonstrated the smallest increase in stress. The most substantial reduction in stress on femur was observed in intramedullary reduction, averaging 21.1%, whereas anatomical and extramedullary reductions displayed reduction rates of 4.1% and 7%, respectively.

In summary, as bone strength diminishes, the force applied to the nail increases, whereas the force exerted on the femur decreases relative to normal bone density. This trend can be attributed to the declining support capacity of the femur when fixed with a nail, which leads to increased loading on the nail. Considering that the
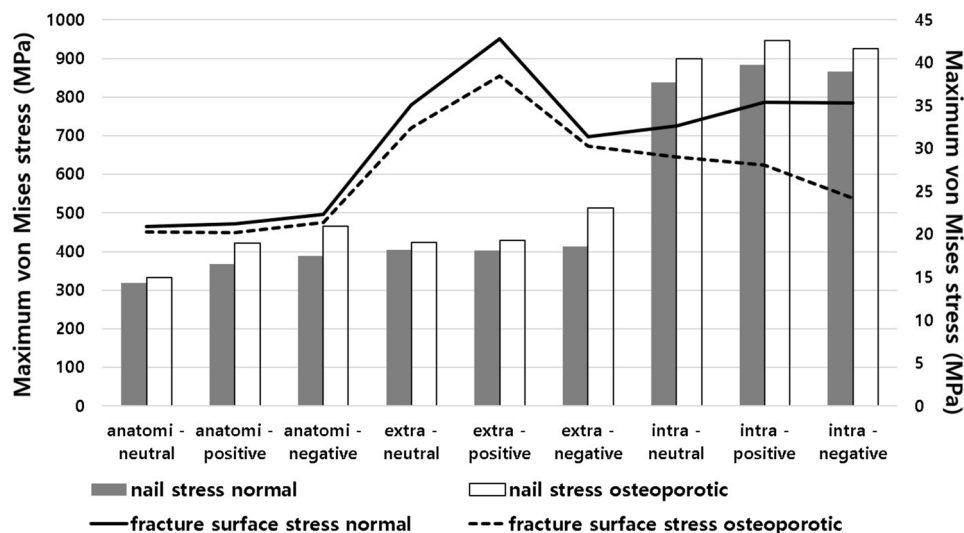
Figure 10. Comparison of maximum von Mises stress between normal and osteoporotic bones.

nail experiences the highest stress during intramedullary reduction, it is inferred that the femur experiences the most significant stress change due to the altered bone strength.

This study has certain limitations that must be acknowledged. First, despite the efforts to simulate the physiological force components around the proximal femur during normal walking, the actual physiological loads in clinical settings may be more intricate and generate greater loads. However, for the FEA performed in this study, only an axial load that mimicked the forces during a single-leg stance was considered appropriate. Second, the study was conducted solely under linear static conditions, focusing on the risk of fixation failure or refracture in the immediate postoperative period. Long-term periodic load FEA was not performed to assess the conditions until osteoclasticity was achieved. Third, the precise interaction among the nail, screw, and bone could not be accurately determined. Additionally, isotropic material properties were used to simulate the human femur. Since recent studies define bone as an anisotropic material for more realistic expression and accurate results, future studies should adopt anisotropic material properties. As a final limitation, the calculation model used to simulate the human body relied on a stable commercial program. In future research, it is necessary to apply computational biology using ODE-based theoretical modeling[30,31]. Therefore, general contact conditions from prior studies on femoral intertrochanteric fractures were utilized, which lacked the ability to model the exact nature of the interactions. Finally, it is important to note that this study relied on FEA as an experimental method, and although it provides valuable insights, clinical evidence from real-world cases remains limited. However, this study contributes by improving fixed stability against intertrochanteric fractures and offers simulations to mitigate the risk of fixation failure.

Notwithstanding these limitations, the primary strength of this study was its ability to simulate the clinical outcomes related to intertrochanteric fractures. It calculates the stress experienced by the implants and femur, and provides valuable insights that are not practically feasible in clinical settings. Moreover, by comparing different reduction methods and bone stiffness values using the same femoral shape, this study offers insights into the selection of appropriate reduction methods.

Conclusion

This study aimed to assess the impact of reduction position on the stability of fixation in surgical management of intertrochanteric fractures using FEA.

In cases where intramedullary reduction was applied, a heightened risk of implant failure was observed due to significantly increased equivalent stress about up to 2.5 times higher on the nail. This risk was notably pronounced in scenarios in which the bone strength was diminished, such as in cases of advanced age or osteoporosis. Conversely, extramedullary reduction demonstrated potential for greater stability compared to anatomical reduction, provided an optimal level of displacement was achieved. When normal bone was reduced to the strength of osteoporotic bone, the fracture surface AMVS of anatomical reduction decreased by 4.1% and the AMVS of the nail increased by 13.1%. Compared with other fracture reductions, the stress change on the femur or nail was the smallest due to the reduced bone strength caused by osteoporosis.

There is no significant difference in the stress received by each part according to the support position (neutral, positive, negative) of the lateral view in the normal bone state. However, when bone density decreased, it was observed that, on an average, the equivalent stress on the nail tended to be lower in the positive support position. Furthermore, the equivalent stress on the femur decreased only in the extramedullary reduction-negative position.

These findings underscore the critical impact of reduction position and bone density on fixation stability. Extramedullary reduction emerged as a potentially favorable approach, particularly when bone density is

compromised, demonstrating relatively consistent stability in both the nail and femur. These insights could significantly inform decision making regarding surgical strategies for intertrochanteric fractures.

Data availability

All data generated or analyzed during this study are available in the main text.

References

1. Wu, H.-F. *et al.* Biomechanical investigation of dynamic hip screw and wire fixation on an unstable intertrochanteric fracture. *Biomed. Eng. Online* **18**, 1–12 (2019).
2. Liang, H. *et al.* Biomechanical study of reduction quality and effects of the medial wall on intertrochanteric fractures based on the new AO classification. *Int. J. Clin. Exp. Med.* **12**(7), 9251–9258 (2019).
3. Kawamura, T. *et al.* Biomechanical evaluation of extramedullary versus intramedullary reduction in unstable femoral trochanteric fractures. *Geriatr. Orthop. Surg. Rehabil.* **12**, 2151459321998611 (2021).
4. Merckaert, S., Hefer, S. & Akiki, A. Unusual complication after intramedullary nailing of an intertrochanteric fracture. *J. Long-Term Effects Med. Implants* **26**, 4 (2016).
5. Kaufer, H. Mechanics of the treatment of hip injuries. *Clin. Orthop. Relat. Res.* **146**, 53–61 (1980).
6. Sonawane, D. V. Classifications of intertrochanteric fractures and their clinical importance. *Trauma Int.* **1**(1), 7–11 (2015).
7. John, B. *et al.* Tip-apex distance and other predictors of outcome in cephalomedullary nailing of unstable trochanteric fractures. *J. Clin. Orthop. Trauma* **10**, S88–S94 (2019).
8. Jia, X. *et al.* The accuracy of intra-operative fluoroscopy in evaluating the reduction quality of intertrochanteric hip fractures. *Int. Orthop.* **44**, 1201–1208 (2020).
9. Chang, S.-M. *et al.* Anteromedial cortical support reduction in unstable pertrochanteric fractures: A comparison of intra-operative fluoroscopy and post-operative three dimensional computerised tomography reconstruction. *Int. Orthop.* **42**, 183–189 (2018).
10. Chang, S.-M. *et al.* Fracture reduction with positive medial cortical support: A key element in stability reconstruction for the unstable pertrochanteric hip fractures. *Arch. Orthop. Trauma Surg.* **135**, 811–818 (2015).
11. Kozono, N. *et al.* Direct reduction may need to be considered to avoid postoperative subtype P in patients with an unstable trochanteric fracture: A retrospective study using a multivariate analysis. *Arch. Orthop. Trauma Surg.* **134**, 1649–1654 (2014).
12. Li, J. *et al.* Medial sustainable nail versus proximal femoral nail antirotation in treating AO/OTA 31–A2.3 fractures: Finite element analysis and biomechanical evaluation. *Injury* **50**(3), 648–656 (2019).
13. Tucker, S. M. *et al.* Parametric finite element analysis of intramedullary nail fixation of proximal femur fractures. *J. Orthop. Res.* **37**(11), 2358–2366 (2019).
14. Shao, Q. *et al.* Positive or negative anteromedial cortical support of unstable pertrochanteric femoral fractures: A finite element analysis study. *Biomed. Pharmacother.* **138**, 111473 (2021).
15. Komatsu, M. *et al.* What is the most fixable intramedullary implant for basicervical fracture and transcervical shear fracture?—A finite element study. *J. Clin. Orthop. Trauma* **34**, 102015 (2022).
16. Wang, Y. C. *et al.* Finite element analysis of mechanical characteristics of internal fixation for treatment of proximal femoral osteolytic lesions in children. *Orthop. Surg.* **15**(2), 628–638 (2023).
17. Lee, P.-Y. *et al.* Biomechanical effect of different femoral neck blade position on the fixation of intertrochanteric fracture: A finite element analysis. *Biomed. Eng.* **61**(3), 331–336 (2016).
18. Kwak, D.-K. *et al.* Effect of the additional anteroposterior blocking screw on nail/medullary canal mismatch after cephalomedullary nailing in unstable pertrochanteric fracture: A finite element analysis. *Bone Jt. Res.* **11**(3), 152–161 (2022).
19. Lee, S. *et al.* Correlation between bone mineral density measured by dual-energy X-ray absorptiometry and Hounsfield units measured by diagnostic CT in lumbar spine. *J. Korean Neurosurg. Soc.* **54**(5), 384–389 (2013).
20. Zhang, Y. *et al.* Effect of screw tunnels on proximal femur strength after screw removal: A finite element analysis. *Orthop. Traumat. Surg. Res.* **108**(8), 103408 (2022).
21. Bayraktar, H. H. *et al.* Comparison of the elastic and yield properties of human femoral trabecular and cortical bone tissue. *J. Biomech.* **37**(1), 27–35 (2004).
22. Kaneko, T. S. *et al.* Relationships between material properties and CT scan data of cortical bone with and without metastatic lesions. *Med. Eng. Phys.* **25**(6), 445–454 (2003).
23. Nalla, R. *et al.* On the influence of mechanical surface treatments—Deep rolling and laser shock peening—On the fatigue behavior of Ti–6Al–4V at ambient and elevated temperatures. *Mater. Sci. Eng. A* **355**(1–2), 216–230 (2003).
24. Rathor, S. *et al.* Effective treatment of femur diaphyseal fracture with compression plate—A finite element and in vivo study comparing the healing outcomes of nailing and plating. *Indian J. Orthop.* **57**(1), 146–158 (2023).
25. Nag, P. & Chanda, S. Biomechanical design prognosis of two extramedullary fixation devices for subtrochanteric femur fracture: A finite element study. *Med. Biol. Eng. Comput.* **59**, 271–285 (2021).
26. Martin, B. Aging and strength of bone as a structural material. *Calcified Tissue Int.* **53**, S34–S40 (1993).
27. Lee, Y.-K. *et al.* Intramedullary nail versus extramedullary plate fixation for unstable intertrochanteric fractures: Decision analysis. *Arch. Orthop. Trauma Surg.* **133**, 961–968 (2013).
28. Schipper, I., Marti, R. & Van der Werken, C. Unstable trochanteric femoral fractures: Extramedullary or intramedullary fixation: Review of literature. *Injury* **35**(2), 142–151 (2004).
29. Turner, C., Wang, T. & Burr, D. Shear strength and fatigue properties of human cortical bone determined from pure shear tests. *Calcified Tissue Int.* **69**, 6 (2001).
30. Jin, J. *et al.* Biphasic amplitude oscillator characterized by distinct dynamics of trough and crest. *Phys. Rev. E* **108**(6), 064412 (2023).
31. Jin, J. *et al.* Quantifying the underlying landscape, entropy production and biological path of the cell fate decision between apoptosis and pyroptosis. *Chaos Solitons Fract.* **178**, 114328 (2024).

Acknowledgements

Author contributions

All authors contributed to the study conception and design. Material preparation, data collection and analysis were performed by CJ, JS, TS, WC, and CL. The first draft of the manuscript was written by CJ and all authors commented on previous versions of the manuscript. All authors read and approved the final manuscript.

Competing interests

The authors declare no competing interests.

Additional information

Correspondence and requests for materials should be addressed to W.C.S. or C.L.

Reprints and permissions information is available at www.nature.com/reprints.

Publisher's note Springer Nature remains neutral with regard to jurisdictional claims in published maps and institutional affiliations.